Kobe University Repository : Kernel

PDF issue: 2025-12-05

Discrete dislocation dynamics study on interaction between prismatic dislocation loop and interfacial network dislocations

Yashiro, Kisaragi
Konishi, Masaaki
Tomita, Yoshihiro

(Citation)
Computational Materials Science,43(3):481-488

(Issue Date)
2008-09

(Resource Type)
journal article

(Version)
Accepted Manuscript

(URL)
https://hdl.handle.net/20.500.14094/90000807

Discrete Dislocation Dynamics Study on Interaction between Prismatic Dislocation Loop and Interfacial Network Dislocations

K. Yashiro[a,*], M. Konishi[b] and Y. Tomita[a]

[a] Graduate School of Engineering, Kobe University, 1-1, Nada, Kobe 657-8501, JAPAN

[b] Student of Graduate School of Engineering, Kobe University, 1-1, Nada, Kobe 657-8501, JAPAN

Abstract

As a series study of the discrete dislocation dynamics (DDD) simulation on the interfacial dislocation network in Ni-based superalloys, we have performed various DDD simulations on the stability of dislocation network and its interaction with a prismatic dislocation loop. Dislocations can't keep its network shape if the line and Burgers vectors are set to the experimental observation, while we can actually obtain stable networks with the vectors and slip plane reported in molecular dynamics (MD) simulations. Then we bump a prismatic dislocation loop into the networks, showing that a mesh knot is replaced by the prismatic loop as reported in our previous MD simulation. The interaction can be explained by the junction formation between the network and prismatic loop, so that we can conclude that any special modeling is not necessary for this interaction between the network and prismatic loop.

Key words: Discrete Dislocation Dynamics, Interfacial Dislocation Network,

Prismatic Dislocation Loop, Ni-based Superalloy, Anti-Phase Boundary

PACS:

1 Introduction

Dislocation motion in the unique microstructure of single crystalline Ni-based superalloys draws keen interest of many researchers, not only the specialists of transmission electron microscopy but also the computational mechanics researchers [1]. Even if the computation couldn't be directly combined to the prediction of the creep curve or creep lifetime, we believe that the computation could give us some useful insight on the hopelessly complicated real phenomena. From such a point of view, we have conducted many molecular dynamics (MD) and discrete dislocation dynamics (DDD) simulations [2-5], density functional theory (DFT) calculations on the lattice instability of Ni and Ni_3Al perfect lattices as well as the anti-phase boundary (APB) energy [6], and even the quasi-continuum (QC) analysis [7].

As an experimental background, network-like misfit dislocations are often found on the rafted γ' plate [1,8,9]. Harada's research group has energetically investigated the characteristics of the misfit dislocation networks, reporting the creep lifetime correlated with its mesh spacing as well as the network formation mechanism [10-12]. There is a missing link, however, for the formation process

* Corresponding author. Tel&Fax: +81-78-803-6303

Email address: yashiro@mech.kobe-u.ac.jp (K. Yashiro[a,*], M. Konishi[b] and Y. Tomita[a]).

URL: http://solid.mech.kobe-u.ac.jp/ (K. Yashiro[a,*], M. Konishi[b] and Y. Tomita[a]).

since it is assumed from the morphology and dislocation characters before and after the creep test. The effect of mesh spacing is also supposed by comparing different superalloys. Thus we have applied our back-force model [4], which is derived from the APB energy between the superpartials in the γ' phase and encoded in the DDD simulation code developed by [13,14], for the cutting phenomena. However, it remains a significant question whether we can treat the misfit dislocation as same as the real dislocation gliding in a mono-lattice. Zhu and Wang[15] have investigated the energy and structure of misfit dislocation networks on the interface between Ni and Ni_3Al single crystals, by changing the crystal orientation in their MD simulations. We have also performed many MD simulations, from the viewpoint of the interaction between the misfit dislocation and the usual dislocation in a mono-lattice [3,5]. The results suggest that we can basically treat the core-interactions within the framework of the dislocation theory, or the Burgers vector problem, while we have also observed the generation of the complicated dislocation structures like the stacking fault tetrahedra (SFT) and the prismatic loop, due to the nucleation of new partial dislocations from the misfit network[5]. On the prismatic dislocation loop, especially, we have also reported that the mesh knot of misfit dislocation network attracts it and changes the network morphology, in the MD simulation of indentation[3]. The prismatic loop may also play an important role in the network formation in real superalloys [10], so that it is of great interest to model the interaction between the misfit dislocation network and a prismatic dislocation loop.

In the present study, various DDD simulations are conducted on the stability of dislocation network on a flat γ/γ' interface and its interaction with a prismatic dislocation loop. Of course it would be a rigorous way to bottom-up

the detail investigation of MD simulations; however, it is so far difficult to combine the results directly to the dislocation theory, due to the insufficient simulation box or the computational limit for real boundary condition. Thus it is rather fruitful to approach the phenomena from both bottom-up and top-down approaches, that is, not only the atomistic scope but also the continuum based dislocation theory. Comparing the MD and DDD result each other, we can judge whether we have to propose a new model for the DDD simulation or not.

2 DDD Formulation and Back Force Model

The DDD simulation code, Micro3D, which is a part of the comprehensive multiscale dislocation dynamics plasticity package, MDDP[14], is used in the present study. The package can treat the eigenstrain problem of the precipitate in the matrix as well as the mirror force from the hetero-phase interface by the superposition of the FEM results; however, we don't perform such coupled analysis of DDD and FEM since the difference in the shear moduli is so little and the main target of this study is the core-level interaction between the interfacial dislocation network and a prismatic loop. According to the formulation by Zbib et al.[13], all the dislocation curves are discretized into many straight line segments of mixed dislocation characters. Then the force acting on a dislocation node is evaluated with the stress field from all the other segments except the two segments include the node itself, according to the following equation;

$$\mathbf{F}_i(\mathbf{p}) = \sum^{X} (\sigma^{D}_{j,j+1}(\mathbf{p}) + \sigma^{a}(\mathbf{p})) \cdot \mathbf{b}_i \times \boldsymbol{\xi}_i + \mathbf{F}_{i-self} \tag{1}$$

where $\mathsf{F_i}(\mathsf{p})$ is the force acting on the node i at the position vector p, $\boldsymbol{\sigma}^{\mathsf{D}}_{\mathsf{j,j+1}}(\mathsf{p})$ is the stress from a straight segment between the node j and $j+1$, $\boldsymbol{\sigma}^{\mathsf{a}}(\mathsf{p})$ the external stress at the position p, $\mathsf{b_i}$ and $\boldsymbol{\xi}_\mathsf{i}$ the Burgers vector and dislocation line vector, respectively. The self force $\mathsf{F_{i-self}}$ is defined by the dislocation curvature at the node i. Then the next position of the node i is obtained by integrating the following equation of motion numerically;

$$m\dot{\mathsf{v}}_\mathsf{i} + \frac{1}{M(T,p)}\mathsf{v_i} = [\mathsf{F_i}]_{\mathsf{glide-component}} \tag{2}$$

here m is the effective mass of dislocation, $\dot{\mathsf{v}}_\mathsf{i}$ and $\mathsf{v_i}$ the acceleration and velocity, respectively, and $[\mathsf{F_i}]_{\mathsf{glide-component}}$ the effective force on the active slip plane. The second term in the left-hand side of the equation represents the damping effect such as phonon drag, with the mobility parameter M which depends on the temperature T and pressure p. The time increment for numerical integration of Eq.(2) is set to $\Delta t = 1.0 \times 10^{-7}$ [s].

In the Micro3D, the short-range or core-level interaction is treated with the "local rule" between dislocation segments [13]. That is, the annihilation, junction and jog formations are judged by the dislocation line, Burgers vector and force, for the segments access each other within a critical distance. We have then proposed another local rule, "back force model", for segments cut into γ' precipitates. A dislocation node receives repulsive force or back force against making the APB, when the next position is in γ' precipitate. Here we ignore the anisotropy of the back force and assume that the back force per unit length, F_b [N/m], acts normal to dislocation line. When a straight segment per unit length travels with the distance n [m] into the γ' phase, it does the work of $F_\mathsf{b}n$ [N] per unit length against the back force. On the other hand, the segment leaves the APB of the width n [m] so that the energy increase

per unit length is evaluated as $E_{\mathsf{APB}} n$ [N], here E_{APB} [J/m^2=N/m] is the APB energy per unit area. Identifying the work with the energy increase, we get $F_{\mathsf{b}} = E_{\mathsf{APB}}$ [N/m]. The trailing dislocation, or trailing superpartial, receives an attractive force of the same magnitude.

3 Stability of Dislocation Network

3.1 Simulation Procedure

The simulation box of 0.38μm×0.38μm×0.38μm shown in Fig. 1(a) and 1(b) is used in the simulations. The lower half is defined as the γ' phase of which shear modulus is 85 [GPa], while the upper one is the γ phase of the modulus 80 [GPa]. The Poisson ratio is set to 0.3 for both phases. Periodic boundary condition is applied in the x and y directions, while the free surface condition is set along the z axis. The crystal orientation is set as usual, the [100], [010] and [001] are the x, y and z axes, respectively. Three network models are considered; Network 1 and 2 have the dislocation lines in the [100] and [010] directions as schematically shown in Fig. 1(a). Zhang et al. [10] have reported that the Burgers vectors of the network are normal to the dislocation lines (edge dislocation) but declined 45 $^\circ$ from the (001) interface, as illustrated in Fig. 1(c) for the case of $[\bar{1}00]$ dislocation lines. That is, the dislocation lines are not on the usual (111) slip planes so that they are sessile dislocations. According to their experimental results, we have set the Burgers vectors of Network 1 alternatively to the [011] and $[01\bar{1}]$ for the $[\bar{1}00]$ dislocation lines, the [101] and $[10\bar{1}]$ for the [010] lines, respectively. Here, the convention for Burgers circuit is adopted, i.e., the sign of Burgers vector is defined on the right-handed

screw rule. For Network 2, we have considered that the misfit dislocation could glide on the (001) interface, so that we have set the (001) interface to the slip plane. Since the Burgers vectors should be parallel to the slip plane and normal to the dislocation line as misfit edge dislocation, they are set to the [010] for the $[\bar{1}00]$ lines as shown in Fig. 1(d), the [100] for the [010] ones, respectively. The last, Network 3, is derived from MD results, i.e. the lines are the [110] and $[\bar{1}10]$, the Burgers vectors are normal to the lines. The slip plane of Network 3 is also set to the (001) plane as same as Network 2, as illustrated in Fig. 1(e). These dislocation networks are located just on the interface in the γ phase side. The mesh spacing is 0.063μm for Network 1, while two mesh spacing are considered for Network 2 and 3, 0.063μm and 0.046μm for the former, 0.066μm and 0.044μm for the later, respectively. The DDD simulations are then performed during $t = 200\Delta t$ without external loading. Here, the interfacial strain between γ and γ' phases is not considered in the present study. Thus the network dislocations feel only the stress field of themselves, if there is no external load. For the precise treatment of interfacial strain, we should consider the eigen strain of the precipitate and perform FEM-DDD coupled simulations; however, as previously mentioned, the main objective of this study is the core-level interaction between dislocation network and a prismatic dislocation loop. Thus we have so far neglected the effect of lattice misfit.

3.2 Result and Discussion

Figure 2 shows the snapshots of dislocations in the calculation of Network 1, with the slip plane as the usual {111} plane. In the figure, the motion is shown

in the 3D bird view and 2D side view, respectively. The dislocations slide away from the interface and can't maintain the initial shape of the network despite of no loading. The roughness of dislocation lines in the γ phase is due to the multiple slip of the [100] dislocation line penetrating many (111) slip planes. No dislocation cuts into the γ' phase because of the back force against the APB.

Figure 3 shows the motion of dislocation in the simulation of Network 1, with the slip plane of the (001), or the interface between γ and γ' phases. The thick black lines indicate the junction segments. Dislocations make junctions at the mesh knots just after starting the calculation as in Fig. 3(b). Then the junction segments grow and coalesce with each other (Figs. 3(c)$\sim$(e)), resulting in the final orientation in the [110] and [$\bar{1}$10] directions, as observed in MD simulations. This change can be explained by the dislocation circuits schematically illustrated in Fig. 4. In the figure, the line directions are indicated with the arrows while its Burgers vectors are written in the Miller's indices. The experimental observation, Fig. 4(a), can be rewritten as Fig. 4(b) where the line directions are alternately defined and corresponding Burgers vectors are also reversed, resulting in a checker-flag arrangement of the clockwise and counter-clockwise circuits. The junctions can be formed as the magnified figure in Fig. 4(c), without any discrepancy, at the mesh knots between the counter-clockwise and surrounding clockwise circuits. The junctions grow so as to extend the circuits, finally the non-circuit mesh vanishes and the network oriented in the [110] and [$\bar{1}$10]. It is also noteworthy that the Burgers vectors of these junctions are parallel to the (001) interface, that is, they don't have the z-component in the Miller's index, while the original Burgers vectors or the experimental observation are out-of-plane from the (001) interface. Thus we

may conclude that the "misfit" dislocation glide in the (001) interface should have the Burgers vector parallel to the interface and also normal to the line, i.e. edge dislocation character, for making the stable network.

The slip plane for Network 2 and 3 is also set on the (001) interface. Figure 5 shows the morphology of the networks after the $t = 200\Delta t$ calculation. Regardless of the network orientation and mesh spacing, all the network is stable and keeps its initial morphology. This is absolutely due to the limitation of continuum based approach; in this DDD simulation we can't consider the lattice misfit nor the crystal anisotropy so that any network could easily exist only if a condition is satisfied, that is, the glide plane is (001) and the Burgers vector is on the interface and normal to the dislocation line, or the edge character. Network 3 is actually observed in many MD simulations and also suitable to the result of Network 1 with the (001) glide plane. Considering the [101] Burgers vectors of usual dislocation in γ phase, the formation mechanism discussed in Figs. 3 and 4 is natural for the interfacial dislocation on the rafted γ' plate. On the other hand, Network 2 might not exist since we can't so far find it in MD simulation; however, we also treat the network in the following section, as an artificial network which can exist in the continuum based DDD framework.

4 Interaction with Prismatic Dislocation Loop

4.1 Simulation Procedure

Prismatic dislocation loop is composed of edge dislocations, of which primal slip plane is not on the same plane. Thus the loop glides along the "prism"

normal to the loop. We have thus modeled the loop as schematically shown in Fig. 6, where the four edge dislocations are indicated with the dashed line on the different slip planes. In the figure, two Thomson's tetrahedrons are connected at Line ab; the near side one is convex upward against the paper surface, the other convex downward. Dislocations A and C are on the different $(1\bar{1}1)$ planes, and Dislocations B and D also on the different $(11\bar{1})$ ones. The Burgers vector is the $[0\bar{1}\bar{1}]$ throughout the loop, normal to all Dislocations A$\sim$D, that is, the loop is composed of edge dislocations.

We have then performed DDD simulations to bump a prismatic dislocation loop into the network dislocations. As shown in Fig. 7, a prismatic loop is located near the interface in the simulation box of Network 3 and 2, of which mesh spacing is 0.066μm and 0.063μm, respectively. The side length of the loop is 0.053μm. The indentation stress is applied on the prismatic loop along the prism direction, to approach the loop to a mesh knot on the network. That is, the dislocation segments of the loop always feel shear force by pushing into the prism piston as illustrated with arrows in Fig. 7. We didn't implement the same simulation on Network 1 with the changed morphology of Fig. 3(f), since it is identical to Network 3 in the dislocation theory but needs many segments before the collision by a prismatic loop.

4.2 Result and Discussion

The interaction between Network 3 and the prismatic loop is shown in Fig. 8. The dashed lines in Figs. 8(a) and 8(b) indicate the prismatic slip plane. In another simulation without network, the loop glides keeping its shape; however, the lower part of the loop, Dislocations B and C in Fig. 8(b), are

attracted by the network. When they first land on the interface, the mesh knot is also attracted and each Dislocations B and C forms a single dislocation by the coalition with two network lines, warp and weft threads, as shown in Figs. 8(c) and 8(d). The interaction is magnified in Figs. 9(a)∼9(d), and the relationships of Burgers vectors are also written in Figs. 9(e) and 9(f), the close-up top view. The legend "a" indicates the apex between Dislocation B and C. As shown in Figs. 9(a) and 9(b), Dislocations B and C touch the network lines, of which directions are the [110] and $[\bar{1}10]$ so that the Burgers vectors are the $[\bar{1}10]$ and [110], respectively, and form the junctions as the result of the following reactions;

$$[\bar{1}10] + [0\bar{1}\bar{1}] = [\bar{1}0\bar{1}], \qquad [110] + [0\bar{1}\bar{1}] = [10\bar{1}] \tag{3}$$

These reactions attract the mesh knot as shown in Fig. 9(e), leading the further reaction between the junction segments and another network lines, according the following relations;

$$[\bar{1}0\bar{1}] + [110] = [01\bar{1}], \qquad [10\bar{1}] + [\bar{1}10] = [01\bar{1}] \tag{4}$$

The Burgers vectors are written in Fig. 9(f). That is, the segments are composed of three dislocations, and the Burgers vector is out-of-plane against the interface. Back to Fig. 8, the upper part of the loop finally touches down on the interface, replacing the mesh knot by a dislocation loop as shown in Figs. 8(e) and 8(f). The shape is same as the initial prismatic loop, however, the Burgers vector is changed so that the loop has the original $[0\bar{1}\bar{1}]$ in the upper part and the conjugate $[01\bar{1}]$ in the lower. This interaction coincide with the MD results so that we conclude that this phenomena can be basically treated in the continuum framework, while it is rather difficult to identify the Burgers vectors in the complicated MD simulation.

Finally we show the dislocation motion in the simulation of Network 2 in Fig. 10. Here, as mentioned in the previous section, it should be noted first that this interaction may not exist in reality. The lower part of the prismatic loop is also attracted by the network as same as Network 3. The dislocations react only with the weft thread, according to the following equation;

$$[010] + [0\bar{1}\bar{1}] = [00\bar{1}] \tag{5}$$

Thus the dislocation still has the Burgers vector normal to the dislocation line while the rest of the loop has that of the original $[0\bar{1}\bar{1}]$.

5 Summary

For understanding of the stability of the interfacial dislocation network and its interaction with a prismatic dislocation loop, we have performed various DDD simulations by encoding our back-force model, or the APB energy in γ' phase, into the Zbib's DDD code. The network dislocation cannot maintain its shape, with the line directions and Burgers vectors observed in the experiments, if we set the slip plane to the usual (111) plane. On the other hand, the dislocations form junctions to orient in the [110] and $[\bar{1}10]$ directions with the glide plane along the (001) interface, as reported in many MD simulations. It is also explained that the out-of-plane $[0\bar{1}\bar{1}]$ Burgers vector is changed to the [110] family, parallel to the interface, by the junction formation without any discrepancy. Then we bump a prismatic dislocation loop into a mesh knot of network dislocations, showing that the mesh knot is replaced by the loop, as reported in our previous MD simulation. We have also shown that this interaction can be explained by the junction formation or the additional

theorem of the Burgers vector. That is, any special modeling is not necessary for this interaction between the misfit dislocation network and prismatic loop.

Acknowledgment

This work was supported financially in part by a Grant-in-Aid for Scientific Research from the Ministry of Education, Culture, Sports, Science and Technology of Japan.

References

[1] T. M. Pollock, and A. S. Argon, Creep Resistance of CMSX-3 Nickel Base Superalloy Single Crystals, Acta Metal. Mater., 40 (1992) 1-30.

[2] K. Yashiro, M. Naito and Y. Tomita, Molecular Dynamics Simulation of Dislocation Nucleation and Motion at γ/γ' Interface in Ni-Based Superalloy, Int. J. Mech. Sci., 44(2002) 1845-1860.

[3] K. Yashiro, J. R. Pangestu and Y. Tomita, Molecular Dynamics Study of Interfacial Dislocation Network at Gamma/Gamma-Prime Interface in Ni-Based Superalloys, Proc. of Third International Conference on Multiscale Materials Modeling, MMM2006, (2006) 582-584.

[4] K. Yashiro, F. Kurose, Y. Nakashima, K. Kubo, Y. Tomita and H. M. Zbib, Discrete Dislocation Dynamics Simulation of Cutting of γ' Precipitate and Interfacial Dislocation Network in Ni-Based Superalloys, Int. J. Plasticity, 22 (2006) 713-723.

[5] K. Yashiro, J. R. Pangestu and Y. Tomita, Structure and Motion of Misfit

Dislocations at Ni/Ni_3Al Interface: Molecular Dynamics Study, Journal of The Society of Materials Science, Japan, 56 (2007) 439-444.

[6] K. Yashiro, K. Yamagami, K. Kubo and Y. Tomita, Ab-initio Lattice Instability Analysis on Ni and Ni3Al Single Crystals, JSME International Journal, 49 (2006) 100-106.

[7] J. R. Pangestu, K. Yashiro and Y. Tomita, Quasicontinuum Analysis on Misfit Dislocations in Ni-based Superalloys, Proceedings of Third Asian-Pacific Congress on Computational Mechanics, (2007) submitted.

[8] M. Kolbe, A. Dlouhy and G. Eggeler, Dislocation Reactions at γ/γ'–Interfaces during Shear Creep Deformation in the Macroscopic Crystallographic Shear System (001)[110] of CMSX6 Superalloy Single Crystals at 1025 $^\circ$C, Mater. Sci. Eng. A246 (1998) 133-142.

[9] V. Sass and M. Feller-Kniepmeier, Orientation Dependence of Dislocation Structures and Deformation Mechanisms in Creep Deformed CMSX-4 Single Crystals, Mater. Sci. Eng. A245 (1998) 19-28.

[10] J. X. Zhang, T. Murakumo, Y. Koizumi, T. Kobayashi, H. Harada and S. Masaki Jr., Interfacial Dislocation Networks Strengthening a Fourth Generation Single-Crystal TMS-138 Superalloy, Metal. Mater. Trans., A, 33A (2002) 3741-3746.

[11] J. X. Zhang, T. Murakumo, H. Harada and Y. Koizumi, Dependence of Creep Strength on the Interfacial Dislocations in a Fourth Generation SC Superalloy TMS-138, Scripta Materialia, 48 (2003) 287-293.

[12] J. X. Zhang, Y. Koizumi, T. Kobayashi, T. Murakumo and H. Harada, Strengthening by γ/γ' Interfacial Dislocation Networks in TMS-162-Toward a Fifth-Generation Single-Crystal Superalloy, Metall. Mater. Trans. 35A (2004) 1911-1914.

[13] H. M. Zbib, M. Rhee and J. P. Hirth, On Plastic Deformation and the Dynamics of 3D Dislocations, Int. J. Mech. Sci., 40 (1998) 113-127.

[14] H. M. Zbib and T. Diaz de la Rubia, A multiscale model of plasticity, Int. J. Plasticity, 18 (2002) 1133-1163.

[15] T. Zhu and C. Wang, Misfit dislocation networks in the γ/γ' phase interface of a Ni-based single-crystal superalloy: Molecular dynamics simulations, Phys. Rev. B, 72 (2005) 014111.

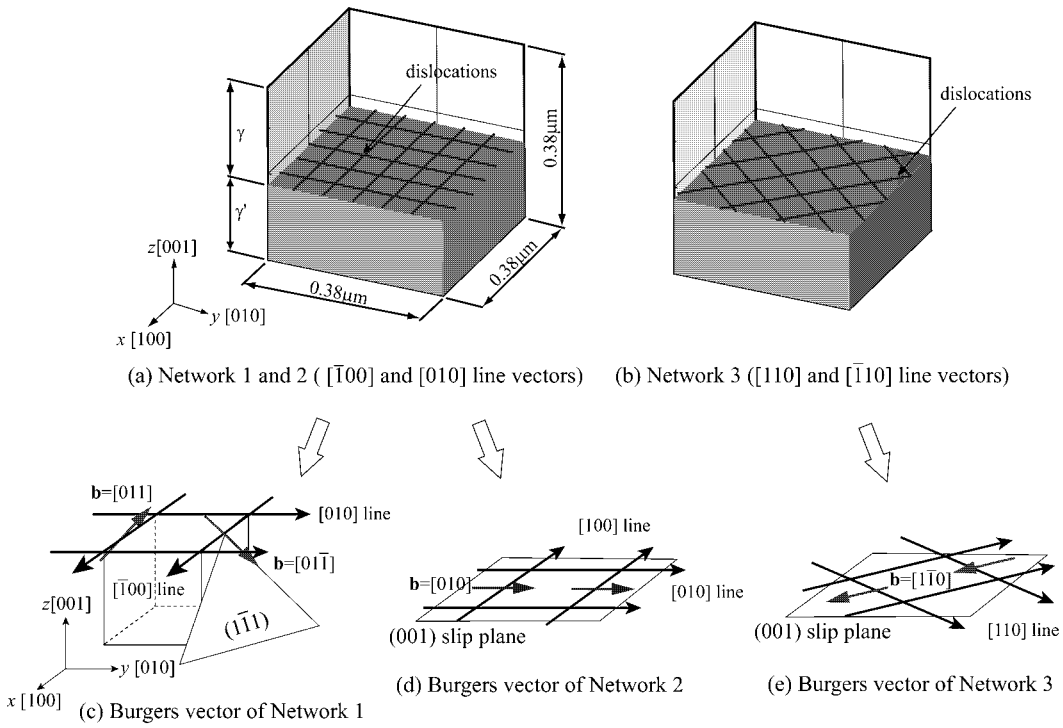

Fig. 1. Simulation cell and dislocation networks.

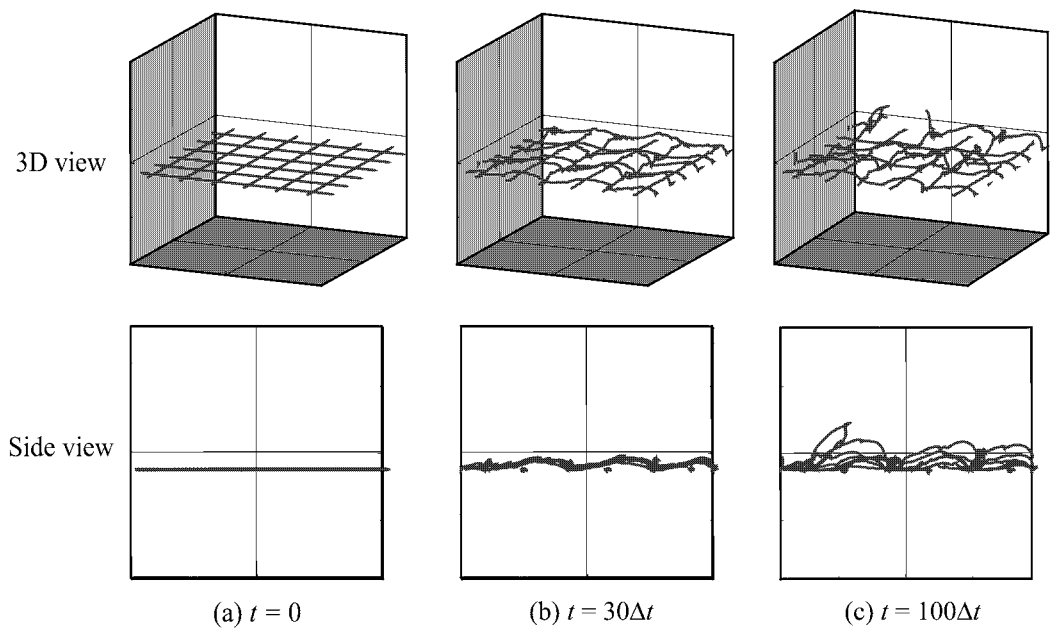

Fig. 2. Motion of dislocations in Network 1 with the (111) slip plane.

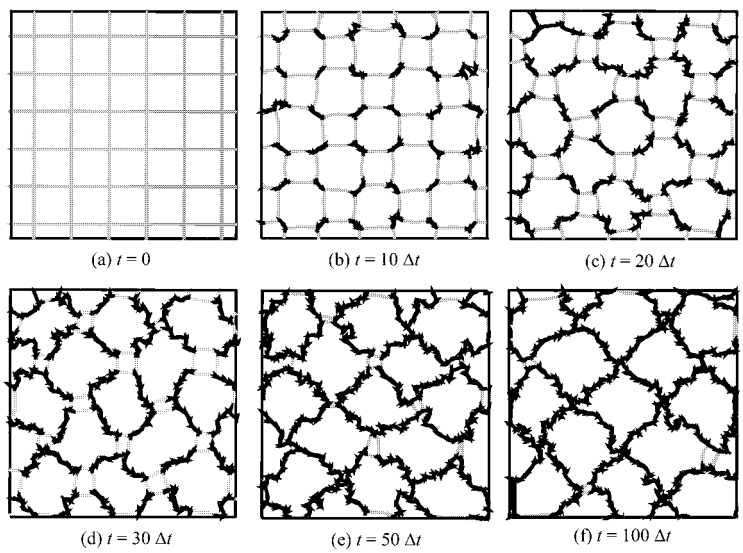

Fig. 3. Motion of dislocations in Network 1 with the (001) slip plane.

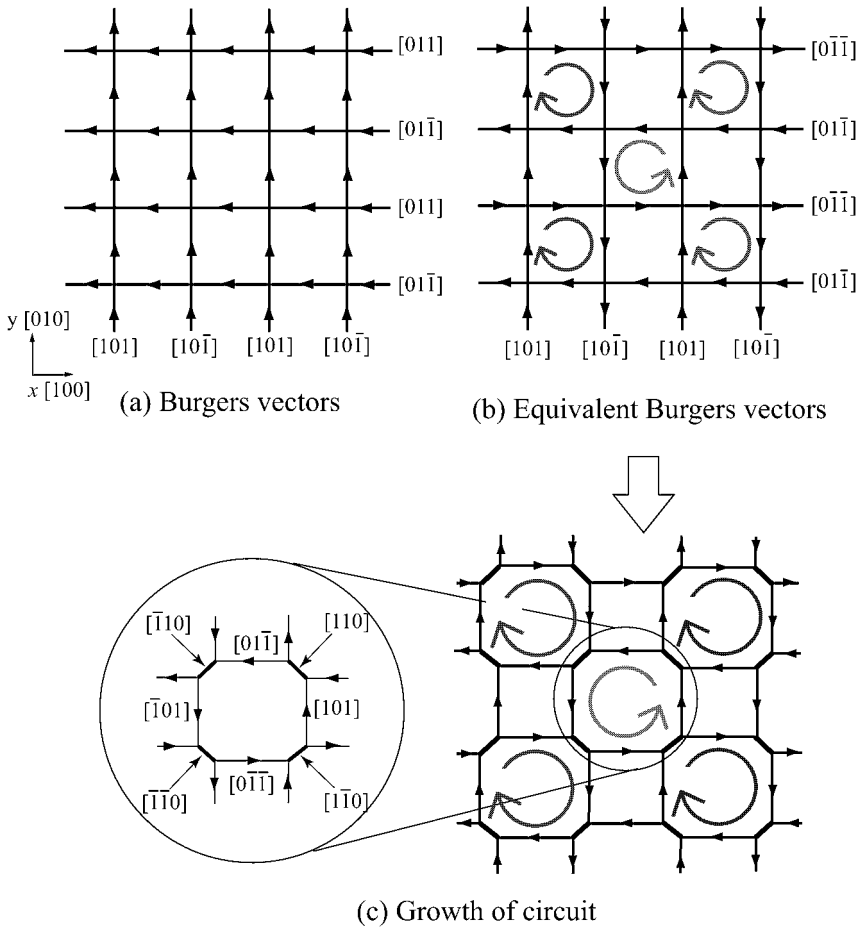

Fig. 4. Shematics of junction formation and its Burgers vectors.

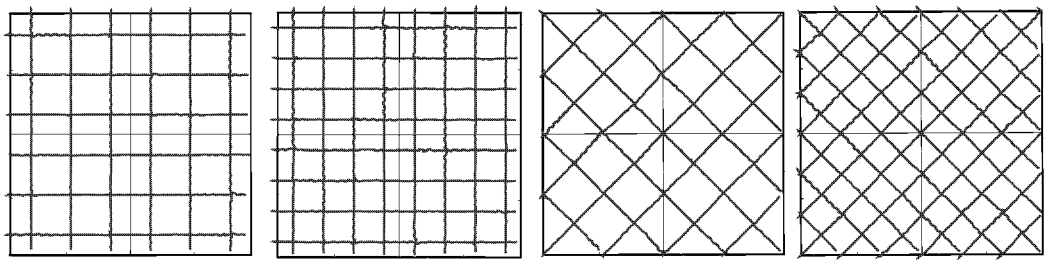

(a) Network 2, d=0.063μm (b) Network 2, d=0.046μm (c) Network 3, d=0.066μm (d) Network 3, d=0.044μm

Fig. 5. Dislocation networks after $t = 200\Delta t$ calculation (Network 2 and 3).

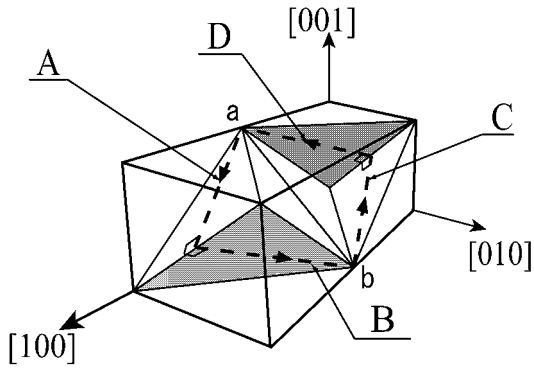

Fig. 6. Schematic of slip plane and prismatic dislocation loop.

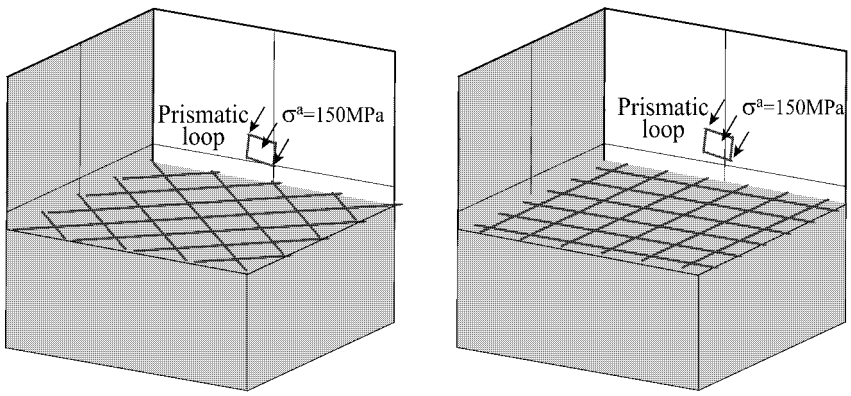

(a) Collision on Network 3 (b) Collision on Network 2

Fig. 7. Simulation models for interaction between network dislocations and a prismatic dislocation loop.

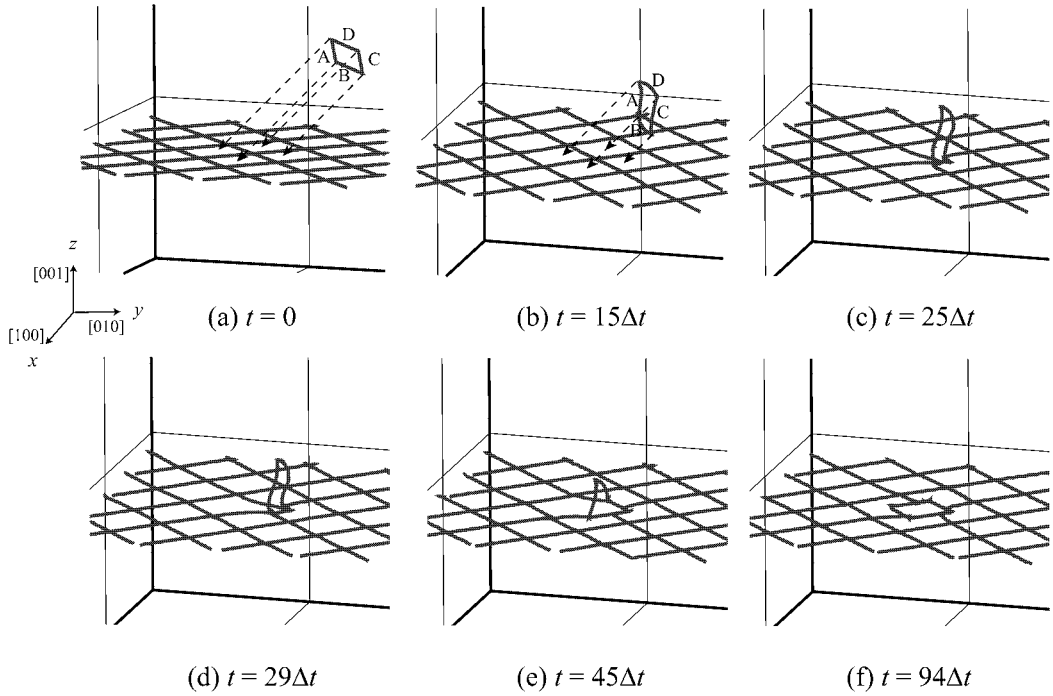

Fig. 8. Morphology change by collision of a prismatic dislocation loop (Network 3).

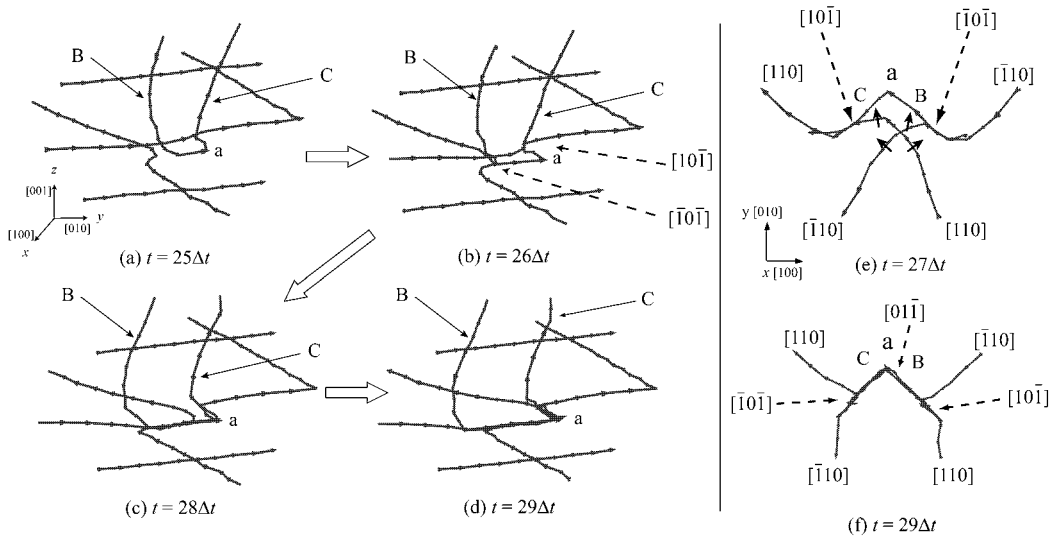

Fig. 9. Morphology change at a mesh knot and its Burgers vectors (Network 3).

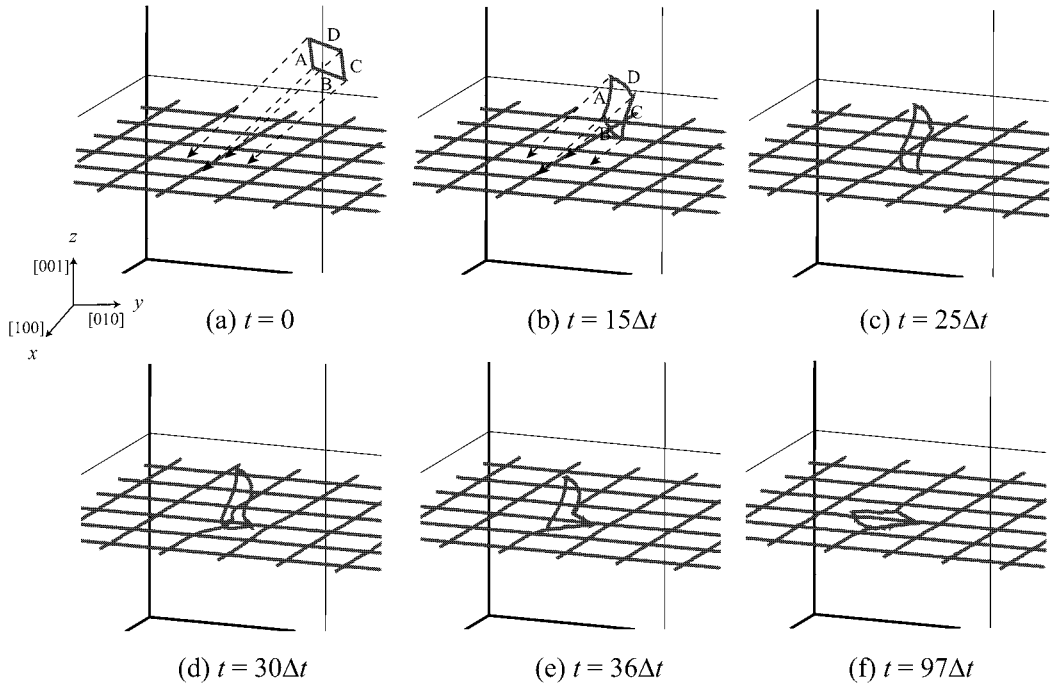

Fig. 10. Morphology change by collision of a prismatic dislocation loop (Network 2).